Original Article

Cardiac compressed sensing real-time cine for the assessment of left ventricular function: a large sample size analysis

Zihan Wang[1#], Zhaozhao Wang[1#], Jing An[2], Ying Yuan[1], Jianing Pang[3], Yi He[1]

[1]Department of Radiology, Beijing Friendship Hospital, Capital Medical University, Beijing, China; [2]Siemens Shenzhen Magnetic Resonance Ltd., Shenzhen, China; [3]Siemens Medical Solutions USA Inc., Chicago, IL, USA

Contributions: (I) Conception and design: Zihan Wang, Zhaozhao Wang, Y He; (II) Administrative support: Y He, J An; (III) Provision of study materials or patients: Y Yuan, J Pang; (IV) Collection and assembly of data: Zihan Wang, Zhaozhao Wang; (V) Data analysis and interpretation: Zihan Wang; (VI) Manuscript writing: All authors; (VII) Final approval of manuscript: All authors.

[#]These authors contributed equally to this work as co-first authors.

Correspondence to: Yi He, MD. Department of Radiology, Beijing Friendship Hospital, Capital Medical University, 95 Yong'an Road, Xicheng District, Beijing 100032, China. Email: heyi139@sina.com.

Background: Segmented cine imaging using a balanced steady-state free precession sequence is the gold standard for accurately quantifying cardiac function and myocardial mass. However, this method suffers from inefficient K-space sampling, resulting in long scan times, and requires multiple breath holds that can be difficult for some patients. Real-time compressed sensing (CS) cine reduces image acquisition time through K-space undersampling and iterative reconstruction, enabling rapid magnetic resonance (MR) imaging. Further large-scale studies need to be conducted to validate its effectiveness. In this study, we assessed image quality and left ventricular (LV) function during the routine clinical use of CS imaging in cardiovascular MR (CMR) to determine the feasibility of using CS cine.

Methods: From April 2022 to March 2023, 242 patients with various heart diseases, including arrhythmia, at outpatient, inpatient, and health examination centers, were consecutively enrolled in this prospective, cross-sectional study and underwent CMR. Two methods [real-time CS cine with free breathing (RTCSCineFB) and conventional breath-hold segmented cine (SegBH)] were used to acquire long- and short-axis cine images of the heart. The total scan time, image quality (Likert score; range, 1–5), LV function parameters, and image fidelity were evaluated for each method.

Results: The study cohort comprised 149 men and 75 women with a mean age of 56.2±15.1 years. The mean ± standard deviation (SD) total scan time was significantly shorter for RTCSCineFB than for SegBH (86.44±31.74 *vs.* 289.81±88.41 s, P<0.001). The overall image quality was slightly lower for RTCSCineFB than for SegBH (P<0.001). The correlations between cardiac function parameters were excellent (0.913–0.984), demonstrating good consistency between the two methods. Both methods were considered equivalent in evaluating LV function and image quality, and showed strong agreement in their diagnostic gradings of ejection fraction (EF) (κ=0.759) and high accuracy.

Conclusions: CS cine assessed LV function with high diagnostic accuracy and enhanced image stability for individuals with arrhythmia while maintaining strong consistency in two methods for EF grading condition.

Keywords: Cardiovascular magnetic resonance imaging (CMR imaging); compressed sensing (CS); left ventricular function (LV function); free breathing (FB); cine

Submitted May 14, 2024. Accepted for publication Oct 15, 2024. Published online Nov 29, 2024.
doi: 10.21037/qims-24-980
View this article at: https://dx.doi.org/10.21037/qims-24-980

Introduction

Cardiovascular magnetic resonance (CMR) is a comprehensive imaging technique that uses multiple parameters and methods to assess cardiac anatomy, function, perfusion, and tissue characteristics in a unified manner. It currently serves as the gold standard for the non-invasive evaluation of cardiac structure and function (1-3). Multi-segmental steady-state free precession is the widely accepted gold standard for left ventricular (LV) assessment (2). Conventional breath-hold segmented cine (SegBH), segmented by retrospective electrocardiogram (ECG)-gated K-space acquisition, offers high spatial resolution, an elevated signal-to-noise ratio, and clear contrast between the blood pool and myocardium. As a result, it is the preferred modality for evaluating myocardial and valve function, and plays crucial roles in the diagnosis and monitoring of various heart diseases (4).

Compared with other imaging methods, current CMR technology is hindered by long scan times that require patients to cooperate by engaging in repeated breath holding to ensure optimal image quality. Occasionally, repeated scanning is necessary due to inadequate patient compliance, particularly when patients experience difficulty with breath holding or exhibit irregular heart rhythms. These issues partially limit the application of CMR. Thus, there is a pressing need to shorten scan times and reduce the patient burden.

Advances in magnetic resonance (MR) technology have enabled various acceleration techniques to be explored for cine imaging. In recent years, compressed sensing (CS) technology has been widely used in rapid MR imaging (4). This imaging technique overcomes the limitations of conventional cine Nyquist sampling by using image sparsity in the transform domain for random K-space sampling and non-linear iterative reconstruction (5). It significantly reduces image acquisition time without the need for breath holding, while also enabling rapid imaging.

CS cine further enhances acceleration by reconstructing complete signals from undersampled K-spaces, and it has been incorporated into the standard protocol guidelines of the CMR Society. CS cine may be a better option for patients with dyspnea, as it decreases the necessity of coordinating patient breathing, thus mitigating this difficulty for the operator. Many heart diseases can cause dyspnea, and the inability of some critically ill patients to cooperate with breathing constraints has limited the application of conventional CMR. However, free breathing (FB) CMR reduces the need for patient cooperation, enabling full CMR examinations in a wider range of patients (e.g., those who cannot tolerate long breath holds) (6). CS cine has been used in some studies to measure ventricular volume and mass, and assess image quality during FB (7-9). However, previous studies have primarily focused on selected populations or specific patient groups with particular diseases, often excluding those with arrhythmia. Consequently, there has been a lack of large-scale investigations regarding this specific population.

The objective assessment of LV ejection fraction (LVEF) is a primary task in CMR. There has been increasing recognition that CMR is the gold standard for assessments of ventricular structure and function. Changes in ejection fraction (EF) manifest late in most cardiac conditions, and serve as an indicator of overall cardiac function (10). The accuracy of CS cine in grading cardiac function and EF remains uncertain; therefore, we sought to validate its grading accuracy.

In this study, we consecutively enrolled patients to determine the feasibility of assessing image quality and LV function using CS cine optimized for acquisition parameters and reconstruction algorithms. Additionally, we conducted a separate subgroup analysis of arrhythmic populations to investigate the utility of CS cine imaging in image quality assessment and to evaluate the accuracy of graded EF measurements obtained from CS cine imaging. We present this article in accordance with the STROBE reporting checklist (available at https://qims.amegroups.com/article/view/10.21037/qims-24-980/rc).

Methods

Study population

In total, 242 patients with various cardiac symptoms at the Beijing Friendship Hospital were consecutively enrolled in this study and underwent CMR between April 2022 and March 2023. The CMR examination has to be discontinued in 18 patients for the following reasons: claustrophobia (n=6), severe dyspnea in the supine position (n=5), the presence of a cardiac implantable electronic device (n=3), a hearing impairment causing an inability to respond to breath-hold commands (n=3), and an urge to urinate (n=1). In total, 224 patients successfully completed the imaging using both methods and were included in the subsequent analysis.

The study cohort comprised 149 men and 75 women

Table 1 Clinical characteristics of patients

Variables	Value (n=224)
Age (years)	56.2±15.1
Gender	
Men	149 (66.5)
Women	75 (33.5)
BMI (kg/m^2)	25.35±3.42
Heart rate (bpm)	68.8±15.1
Clinical diagnosis	
Coronary artery disease	128 (57.1)
Occasional arrhythmias	39 (17.4)
Cardiac symptoms without organic disease	22 (9.8)
Hypertrophic cardiomyopathy	12 (5.4)
Heart failure	9 (4.0)
Myocarditis	6 (2.7)
Dilated cardiomyopathy	3 (1.3)
Valvular heart disease	2 (0.9)
Hypertensive heart disease	2 (0.9)
Cardiac tumor	1 (0.4)

Results are shown as mean ± SD or number (%). BMI, body mass index; SD, standard deviation.

Table 2 Parameters for conventional and CS cine imaging

Parameters	SegBH	RTCSCineFB
Echo spacing (ms)	3.32	3.21
Echo time (ms)	1.46	1.41
Flip angle (°)	50–70	45–60
Spatial resolution (mm^2)	1.5×1.5	1.8×1.8
Temporal resolution (ms)	39.84	38.52
FOV (mm^2)	340×320	340×320
Matrix	224×210	192×180
Bandwidth (Hz/pixel)	962	920
Slice thickness/gap (mm)	8/0	8/0
Cardiac phases (n)	25	25
Acceleration factor	3	11
ECG mode	Retrospective gating	Adaptive triggering

CS, compressed sensing; SegBH, breath-hold segmented cine; RTCSCineFB, real-time compressed sensing cine with free breathing; FOV, field of view; ECG, electrocardiogram.

with a mean age of 56.2±15.1 years, and a mean heart rate of 68.8±15.1 beats/min. The clinical diagnoses were coronary artery disease (n=128), occasional arrhythmias (n=39), cardiac symptoms without organic disease (n=22), hypertrophic cardiomyopathy (n=12), heart failure (n=9), myocarditis (n=6), dilated cardiomyopathy (n=3), hypertensive heart disease (n=2), valvular heart disease (n=2), and cardiac tumor (n=1) (*Table 1*). All the participants were scheduled to undergo imaging using both SegBH (the reference method) and RTCSCineFB. All participants provided written informed consent to participate in the study. The Ethics Committee of the Beijing Friendship Hospital (No. 2021-P2-418-01) approved the study protocol. The study was conducted in accordance with the Declaration of Helsinki (as revised in 2013).

Imaging protocol

MR imaging was performed on a 3-T scanner (Siemens Healthineers, Erlangen, Germany) using an 18-channel phased-array surface coil. All patients underwent imaging with SegBH as the conventional reference method. Images were collected during breath holds using a generalized autocalibration partial parallel acquisition acceleration technique. Real-time CS cine with FB (RTCSCineFB) was performed with the patients breathing freely. The images for each patient were sequentially acquired using SegBH and RTCSCineFB prior to the administration of the contrast agent. The imaging range covered the entire LV from the base to the apex. Long-axis cine images included two-, three-, and four-chamber views; short-axis cine images comprised short-axis views. The slices were equidistant and parallel to each other. The number of slices ranged from eight to 14; the number was adjusted based on the heart size and clinical indications for each patient in accordance with system standards. For post-processing, all cine images were acquired in 25 cardiac phases. The total scan time was recorded for each technique. The imaging parameters were similar for both methods (*Table 2*).

The FB adaptive ECG-triggered RTCSCineFB scans were performed immediately after the conventional SegBH scans. RTCSCineFB data acquisition used a real-time cardiac cine sequence with sparse, incoherent Cartesian K-space sampling, and balanced steady-state free precession readout. This readout format was achieved with a random distribution of readouts on the Cartesian grid in K-space (11,12). In this protocol, acquisition was triggered by the R peak on the ECG. Adaptive triggering was implemented to

capture the complete cardiac cycle. The "real" number of cardiac phases depended on each patient's heart rate, which led to between-slice variation in the number of cardiac phases acquired. RTCSCineFB used data from one R-R interval to reconstruct whole image phases for each slice. Image reconstruction was performed using a non-linear, iterative SENSE-type approach that implemented spatiotemporal regularization via redundant Haar wavelets (13). The corresponding cost function was solved by Fast Iterative Shrinkage-Threshold Algorithm optimization that consisted of a gradient descent step for the quadratic terms, and an evaluation of the proximal operator. All reconstructions were performed in real time, and images were directly transmitted to workstations for subsequent analysis.

Image quality assessment

Two experienced radiologists, blinded to the imaging method (SegBH *vs.* RTCSCineFB), assessed the overall image quality. If a difference of opinion arose between the two radiologists, a third, more senior radiologist analyzed or scored the image. Artifact presence and endocardial border clarity were evaluated using a 5-point rating scale on which 1 represented no diagnostic value, 2 represented poor quality with some acceptable artifacts, 3 represented good quality with minimal and non-impacting artifacts, 4 represented excellent quality without significant artifacts, and 5 represented outstanding quality with clear blood pool contrast and no artifacts (8). An image quality score ≥3 was considered diagnostically significant, and images with a score ≥3 were included in the subsequent analyses. Image quality was evaluated in the subgroup analyses according to the presence or absence of arrhythmia. The arrhythmia group was further divided into patients with clinically diagnosed arrhythmia and patients exhibiting irregular heartbeats during image acquisition defined as an R-R interval standard deviation (SD) greater than 10% of the R-R interval (7).

Because the CS reconstruction process continuously eliminates noise, the conventional signal-to-noise ratio measurement cannot be applied (14,15). Therefore, blood-to-myocardial contrast (BMC) was used to assess image contrast in the short-axis cine images for both cohorts. The signal intensity values for the blood pool and myocardium were acquired from the short-axis images at the mid-ventricular level during end diastole (ED). The region of interest, covering approximately two-thirds of the ventricular septum width, represented myocardial pixel density. A similarly sized region of interest (radius ≥2 mm) was placed at the center of the LV cavity, excluding papillary muscles and chordae tendineae, to accurately measure the blood pool signal. BMC was calculated as the signal ratio between these two regions of interest (8).

The edge sharpness of the endocardial blood pool boundary was evaluated in the acquired images as follows. A line perpendicular to the middle of the interventricular septum was drawn, extending from the septum to the LV blood pool boundary, crossing both the myocardium and the blood pool. Using MATLAB 2023 software the signal intensity distribution along this line was measured, and the local maximum and minimum intensity values (I_{max} and I_{min}) were observed, corresponding to the blood pool and myocardial pixel intensities, respectively. The points corresponding to 20% and 80% of the difference between the I_{max} and I_{min} were then identified. The distance between these two points was regarded as d, and edge sharpness was defined as the reciprocal of d (ε, mm^{-1}) (16,17).

Scan time assessment

Scan time assessment comprised the calculation of the total scan duration, including the breath commands, breath-holding time, breath-hold intervals, imaging time, and reconstruction time.

Assessment of cardiac morphology

Cardiac function in all short-axis cine images was quantified on a CVI42 workstation (Circle Imaging Systems, Calgary, Canada) by an experienced CMR physician under the supervision of a senior physician. Basal and apical slices were automatically identified by artificial intelligence; the LV endocardium and epicardium were automatically traced at ED and end systole (ES). The automatic results were manually adjusted with careful consideration of the following principles: ED was defined as the phase with the largest blood pool area at the mid-ventricular level; ES was defined as the phase with the smallest blood pool area. During the establishment of the basal slice, interactive reference to long-axis images enabled the tracking of changes in blood pool size and myocardial thickness (from ED to ES). Ventricular volume included the outflow tract, intracardiac papillary muscles, and myocardial trabeculae. LV volume was calculated using Simpson's rule to derive the following morphological and functional parameters: LV end-diastolic volume (LVEDV); LV end-systolic volume

(LVESV); LV stroke volume (LVSV); and LVEF. To determine the myocardial LV mass (LVM), the myocardial density (1.05 g/cm^2) was multiplied by the volume enclosed between the LV endocardium and epicardium (18).

Assessment of EF grading

The EF values obtained from both methods were categorized into the following three grades: grade 1 (EF <40%); grade 2 (40%≤ EF <50%); and grade 3 (EF ≥50%). To determine the accuracy of each method, the EF values of the two methods were grouped into different intervals to investigate whether the EF classifications were consistent between the methods, and whether there were any changes in classifications.

Statistical analysis

SPSS 23 and MedCalc 20 software were used for the statistical analysis. The results for all continuous variables of cardiac function (LVEDV, LVESV, LVSV, LVEF, and LVM) and their differences are expressed as the mean and SD. Data normality was visually assessed through histogram and Q-Q plot analyses. No significant deviations from normality were observed; therefore, paired *t*-tests were used to determine statistical significance. P values <0.05 were considered statistically significant. Pearson correlation coefficients (r) were used to assess the associations between individual parameter values obtained from each method. Bland-Altman plots were generated to evaluate the consistency between the two methods. In accordance with the method of Zange *et al.* (19), the equivalence boundary was defined as the 95% tolerance interval for intra-observer differences within the same method, with 95% coverage. If the discrepancies between two methods fell within the range of deviations observed by the same observer using the same method for measurement, they were considered equivalent. An equivalence limit for LV was established as follows: using SegBH short-axis data from 224 patients, discrepancies in the quantified parameters between the observers were computed and graphically depicted by the same assessor on two separate occasions with an interval of >2 months. If the differences exhibited a sufficiently normal distribution, the equivalence limit was regarded as ±1.96 times the maximum within-observer SD of the two methods. If the 95% confidence intervals (CIs) of the differences between the two methods fell completely within the 95% tolerance interval, cardiac function measurement was considered equivalent for both methods. The *t*-test was used to compare the image quality scores, BMC, edge sharpness, and imaging time variables between the two methods. The Kappa test was used to examine consistency in EF grading between the methods. The patients were divided into two groups for the subgroup analysis based on the presence of arrhythmia. The subgroup which analysis the image quality scores, BMC and edge sharpness was conducted in the same statistical method as non-subgroup analysis described above.

Results

Study population

In total, 224 participants were included in our study and successfully underwent both types of cine imaging. Subsequently, based on the presence or absence of arrhythmia diagnosed clinically or detected during the MR examination (using the reference standard criteria for arrhythmia detection), the participants were divided into two groups; one group comprised those with cardiac rhythm abnormalities (n=53), and the other group comprised those without any heart rhythm irregularities (n=171).

Image quality

Image quality scoring, BMC, and edge sharpness measurements were determined for all 224 patients. RTCSCineFB had lower overall image quality than SegBH (with scores of 4.10±0.59 and 4.37±0.92, respectively). However, the mean image quality scores for both methods fell within the diagnostically acceptable range. Research has shown that an image with a quality score of ≥3 exhibits sufficient diagnostic quality (20). RTCSCineFB acquired more diagnostically acceptable images than SegBH [222 (99.11%) *vs.* 213 (95.09%) images, respectively] (*Table 3*).

The patients were divided into subgroups for the subgroup analysis. Of the 224 patients, 53 (23.66%) had arrhythmia. In the arrhythmia group, RTCSCineFB had higher overall image quality than SegBH (4.11±0.72 *vs.* 3.77±1.15 scores, respectively) (*Figure 1*). Additionally, diagnostic quality was achieved in 52 (98.11%) and 44 (83.02%) images acquired by RTCSCineFB and SegBH, respectively. Notably, all the acquired data remained usable because while nine SegBH images failed to meet the diagnostic standards for quality, the corresponding RTCSCineFB images met the diagnostic standards. In

Table 3 Image quality assessment and subgroup analysis in the study population

Parameters	All patients (n=224)			Arrhythmia group (n=53)			Non-arrhythmia group (n=171)		
	SegBH	RTCSCineFB	P	SegBH	RTCSCineFB	P	SegBH	RTCSCineFB	P
Image quality score	4.37±0.92	4.10±0.59	<0.001	3.77±1.15	4.11±0.72	<0.001	4.55±0.75	4.10±0.55	<0.001
Image interpretability rate (score ≥3)	95.09 (213/224)	99.11 (222/224)	–	83.02 (44/53)	98.11 (52/53)	–	98.83 (169/171)	99.42 (170/171)	–
BMC	4.05±0.98	2.14±0.48	<0.001	3.99±1.15	2.21±0.60	<0.001	4.07±0.93	2.12±0.43	<0.001
Edge sharpness	0.530±0.223	0.335±0.151	<0.001	0.532±0.199	0.357±0.159	<0.001	0.529±0.231	0.327±0.147	<0.001

Results are shown as mean ± SD or % (number/total). SegBH, breath-hold segmented cine; RTCSCineFB, real-time compressed sensing cine with free breathing; BMC, blood-to-myocardial contrast; SD, standard deviation.

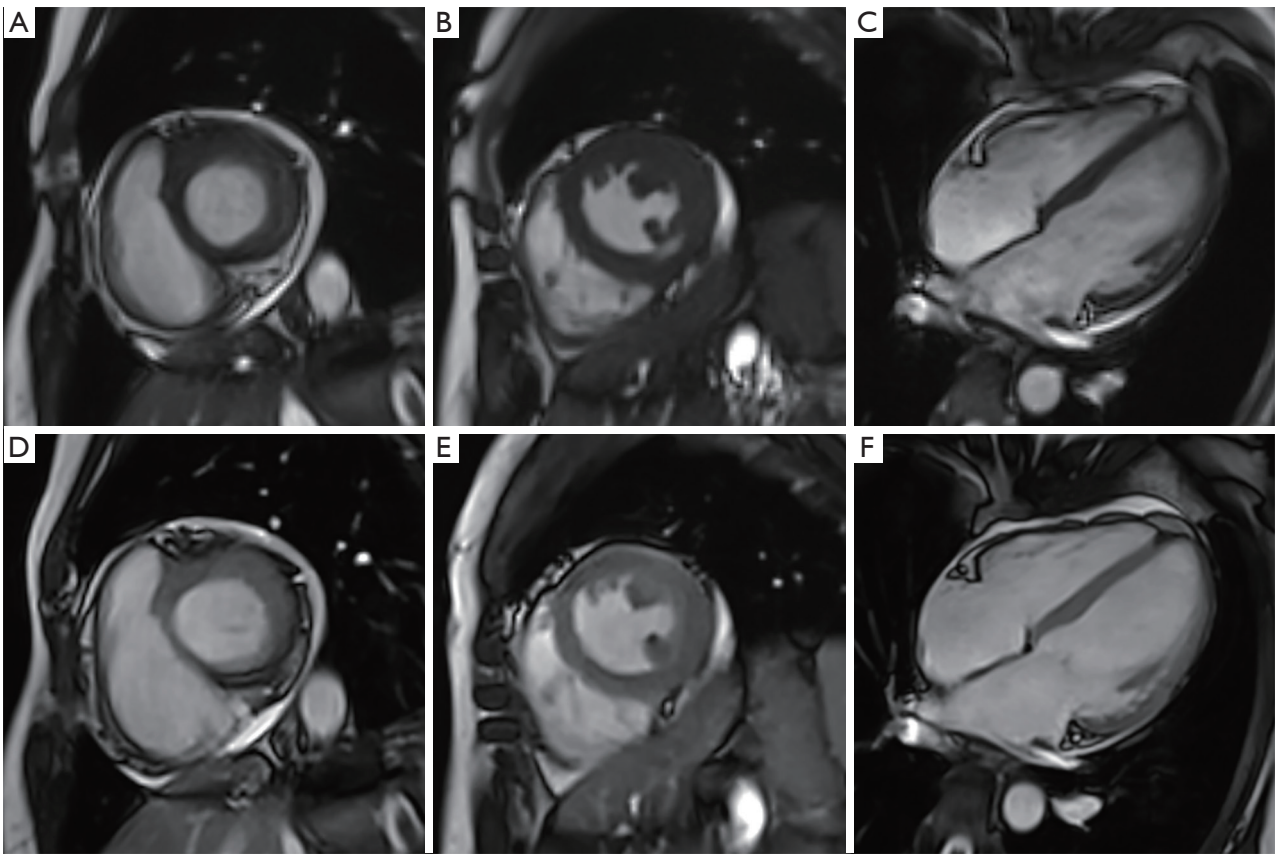

Figure 1 Short-axis and long-axis cine images obtained via the two methods in a patient with cardiac arrhythmia. (A-C) Short-axis base, middle, and long-axis four-chamber views of the LV obtained by SegBH. (D-F) Corresponding short-axis and long-axis views obtained by RTCSCineFB. Both methods demonstrated excellent image quality, with a rating of 5 points. SegBH, breath-hold segmented cine; RTCSCineFB, real-time compressed sensing cine with free breathing.

the non-arrhythmia group, the overall image quality of RTCSCineFB was lower than that of SegBH (4.55±0.75 *vs.* 4.10±0.55 for SegBH *vs.* RTCSCineFB, respectively) (*Table 3*).

BMC differed significantly between the two methods, such that SegBH exhibited higher values (4.05±0.98 pixel^{-1}) than RTCSCineFB (2.14±0.48 pixel^{-1}). In the arrhythmia group, SegBH also exhibited higher BMC (3.99±1.15 pixel^{-1}) than RTCSCineFB (2.21±0.60 pixel^{-1}). Similarly, in the non-

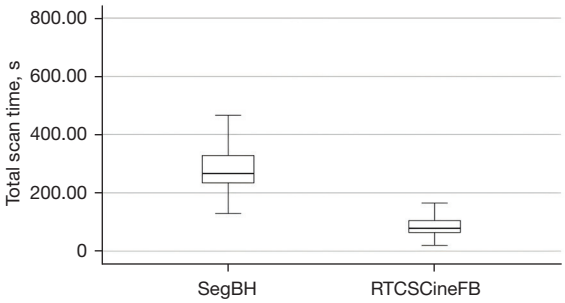

Figure 2 Box plots displaying the mean scan duration in seconds for SegBH and RTCSCineFB images. The upper and lower bounds of the box plot represent the maximum and minimum values; lines indicate the 25th percentile, median, and 75th percentile (in ascending order). SegBH, breath-hold segmented cine; RTCSCineFB, real-time compressed sensing cine with free breathing.

arrhythmia group, SegBH had higher BMC (4.07±0.93 pixel^{-1}) than RTCSCineFB (2.12±0.43 pixel^{-1}).

SegBH had a higher edge sharpness coefficient at the ED (εSegBH: 0.530±0.223 pixel^{-1}) than RTCSCineFB (εRTCSCineFB: 0.335±0.151 pixel^{-1}, P<0.001). In the arrhythmia group, SegBH again had higher edge sharpness (0.532±0.199 pixel^{-1}) than RTCSCineFB (0.357±0.159 pixel^{-1}). This difference persisted in the non-arrhythmia group, such that SegBH had higher edge sharpness (0.529±0.231 pixel^{-1}) than RTCSCineFB (0.327±0.147 pixel^{-1}).

Scan time

The total scan time differed significantly between the two methods for all 224 patients. Specifically, the total time was significantly shorter for RTCSCineFB (86.44±31.74 s) than for SegBH (289.81±88.41 s, P<0.001) (*Figure 2*).

LV function parameters and mass

The cardiac function parameters and myocardial mass obtained from the RTCSCineFB short-axis images were compared with those obtained from conventional SegBH. When quantifying LV function in the short axis, both the RTCSCineFB and SegBH measurements showed mean relative error values <5%. Based on Zange's equivalence test (*Table 4*, *Figure 3*), these two methods appeared comparable. The LV function parameters and mass (represented by the black line in *Figure 3*) fell within their respective 95% tolerance intervals (indicated by the gray shaded area in *Figure 3*); no clinically significant differences were detected.

The correlation analysis revealed strong correlations between RTCSCineFB and SegBH for all cardiac function parameters (r>0.91, P<0.001) (*Table 4*, *Figure 4*). The Bland-Altman analysis showed strong agreement between LV parameters obtained by RTCSCineFB and SegBH (*Figure 4*). These differences were clinically acceptable; however, we observed the following trends: RTCSCineFB slightly overestimated LVEDV and LVESV (−3.64±10.41 and −5.14±8.29 mL, respectively), but slightly underestimated LVSV, LVEF, and LVM (1.75±9.78 mL, 2.61%±5.78%, and 3.29±10.88 g, respectively).

EF grading

The results showed that the EF grading diagnoses of the two methods were consistent for 186 participants (83.04%) and inconsistent for 38 participants (16.96%). Overall, the weighted kappa coefficient κ of the two methods was 0.759 (95% CI: 0.685–0.834; P<0.001), indicating strong agreement (*Tables 5*,*6*).

Discussion

Our study cohort comprised a diverse group of consecutively enrolled patients with various cardiovascular diseases, including arrhythmia, consistent with real-world clinical practice. When assessing image quality among all 224 patients, the conventional SegBH method performed better than the RTCSCineFB method in this study. This difference was even more pronounced in the largest subgroup (of non-arrhythmic patients). However, in the arrhythmia group, RTCSCineFB showed superior image quality compared with the conventional segmented method, resulting in a higher score in the subgroup analysis. In all groups, RTCSCineFB consistently produced a higher percentage of images that met the diagnostic quality standards than SegBH. Thus, RTCSCineFB consistently achieved stable image quality, especially in patients with arrhythmias. The equivalence test demonstrated strong agreement between the conventional method and RTCSCineFB in terms of quantifying all cardiac function parameters. Further, both methods showed strong consistency in EF grading diagnoses. A significant reduction was also observed in total imaging time by CS cine compared with conventional segmented cine.

Conventional cardiac function cine imaging requires multiple breath holds, which can often cause discomfort

Table 4 LV function parameters and mass

Parameters	SegBH	RTCSCineFB	Difference	95% TI (±)[†]	CI within 95% TI (yes/no)	r[‡]	P
LVEDV (mL)				8.53	Yes	0.981	<0.001
Mean ± SD	136.26±53.93	139.90±51.74	−3.64±10.41				
95% CI	129.16 to 143.36	133.09 to 146.71	−5.01 to −2.27				
LVESV (mL)				7.82	Yes	0.984	<0.001
Mean ± SD	66.31±46.40	71.73±47.24	−5.14±8.29				
95% CI	60.20 to 72.42	65.51 to 77.95	−6.51 to −4.32				
LVSV (mL)				8.68	Yes	0.913	0.008
Mean ± SD	69.93±23.75	68.18±22.82	1.75±9.78				
95% CI	66.80 to 73.06	65.18 to 71.19	0.46 to 3.04				
LVEF (%)				5.88	Yes	0.925	<0.001
Mean ± SD	54.26±14.64	51.66±15.05	2.61±5.78				
95% CI	52.33 to 56.19	49.67 to 53.64	1.84 to 3.37				
LVM (g)				12.41	Yes	0.958	<0.001
Mean ± SD	116.05±37.74	112.77±37.71	3.29±10.88				
95% CI	111.08 to 121.02	107.80 to 117.73	1.85 to 4.72				

[†], 95% TI based on 1.96 times SD. [‡], Pearson's correlation coefficient. LV, left ventricular; SegBH, breath-hold segmented cine; RTCSCineFB, real-time compressed sensing cine with free breathing; TI, tolerance interval; LVEDV, left ventricular end-diastolic volume; SD, standard deviation; CI, confidence interval; LVESV, left ventricular end-systolic volume; LVSV, left ventricular stroke volume; LVEF, left ventricular ejection fraction; LVM, left ventricular mass.

to patients during CMR examinations. CS technology overcomes the need for ECG-gated synchronization by collecting synchronous data using K-space undersampling and iterative reconstruction techniques, thereby significantly increasing image acquisition speed, reducing breath-holding duration, and entirely eliminating the necessity of breath holding. When conventional methods are used for arrhythmia patients, artifacts occur; however, the application of the CS method during FB effectively addresses is issue, and thus eliminates the need for repeated scans and additional scanning time. This approach enables high-quality diagnostic images to be obtained in a single scan, avoiding the need of repeat scans, and allowing simultaneous subsequent scans to be acquired during RTCSCineFB reconstruction. Consequently, it minimizes general delays during CMR examinations and significantly reduces the total acquisition time. Our study showed the feasibility of implementing this method in a busy clinical setting.

Previous studies have shown that the CS method effectively reduces imaging time and provides reliable quantitative results for cardiac function assessment, although with slightly lower image quality relative to conventional segmented cine (14,20,21). These observations are consistent with our results. The subjective overall image quality score for the entire population was slightly lower with the CS method than with the conventional segmented method, but the mean score remained diagnostically acceptable (≥3). Moreover, a higher percentage of images acquired with the CS method met diagnostic quality standards, indicating greater stability in image acquisition, and minimizing the risk of obtaining non-diagnostic images. In both the overall population and subgroup analyses, RTCSCineFB demonstrated superior image stability than the conventional SegBH method. This superiority was evident in the higher percentage of patients who had image quality scores ≥3 with RTCSCineFB, highlighting its consistent ability to obtain more stable images. This stability advantage was particularly pronounced in the arrhythmia group. In fact, the image quality score for RTCSCineFB slightly surpassed that of SegBH in the arrhythmia subgroup analysis (4.14±0.69 *vs.*

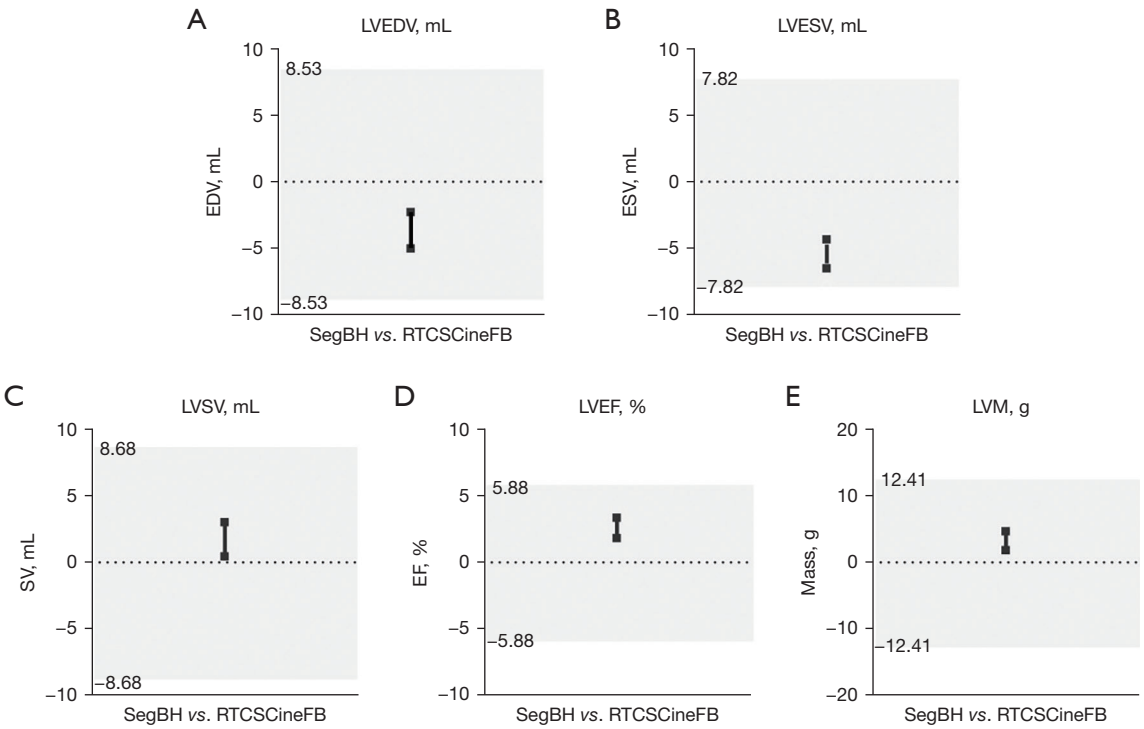

Figure 3 Equivalence testing for the left ventricle. Equivalence assessment for LVEDV (A), LVESV (B), LVSV (C), LVEF (D), and LVM (E). Measurements between the two methods are considered equivalent when the 95% CI for the difference between methods (represented by black lines; the upper and lower limits are denoted by squares) falls within the 95% tolerance interval (indicated in gray). LVEDV, left ventricular end-diastolic volume; EDV, end-diastolic volume; SegBH, breath-hold segmented cine; RTCSCineFB, real-time compressed sensing cine with free breathing; LVESV, left ventricular end-systolic volume; ESV, end-systolic volume; LVSV, left ventricular stroke volume; SV, stroke volume; LVEF, left ventricular ejection fraction; EF, ejection fraction; LVM, left ventricular mass; CI, confidence interval.

3.78±1.12). Similarly, several other studies (7,22) have also shown the potential for improved image quality in patients with arrhythmia. In summary, our results suggest that the use of RTCSCineFB would result in more stable image quality in all cardiac patients. In patients with arrhythmia, the use of CS methods can further enhance image quality, which is particularly beneficial when breath holding is challenging. Such methods can serve as rapid tools for routine clinical use or regular follow-up examinations.

Quantitative measurement of ventricular function is essential in clinical practice. CMR is widely recognized as the most reliable method for evaluating cardiac function among various imaging modalities (23). Even in patients with irregular ventricular morphology, CMR using the Simpson method does not rely on any geometric model, making it suitable for assessments of cardiac function, volume, and quality. The findings of the present study align with previous research that has demonstrated that CS methods can accurately assess LV function in clinical practice (9,12,15,24). While most studies have reported strong consistency between CS and traditional cine in quantitative measurements, some parameters display persistent disparities. We found that CS cine exhibits excellent consistency and correlations with conventional methods in the assessment of LV volume and function measurements during FB, thereby establishing its reliability for ventricular function evaluation while significantly reducing or eliminating the need for breath holding. Although statistically significant differences were observed in the LVEDV, LVESV, LVSV, LVEF, and LVM between the two methods, these discrepancies were minimal and fell within clinically acceptable limits. We attribute these measurement variations to intra-observer variability. Therefore, we conclude that such differences should not hinder the routine clinical application of either method.

Compared with the conventional breath-hold method, the CS method tends to lead to increased LVEDV and LVESV, as reported by other researchers (8). We hypothesize

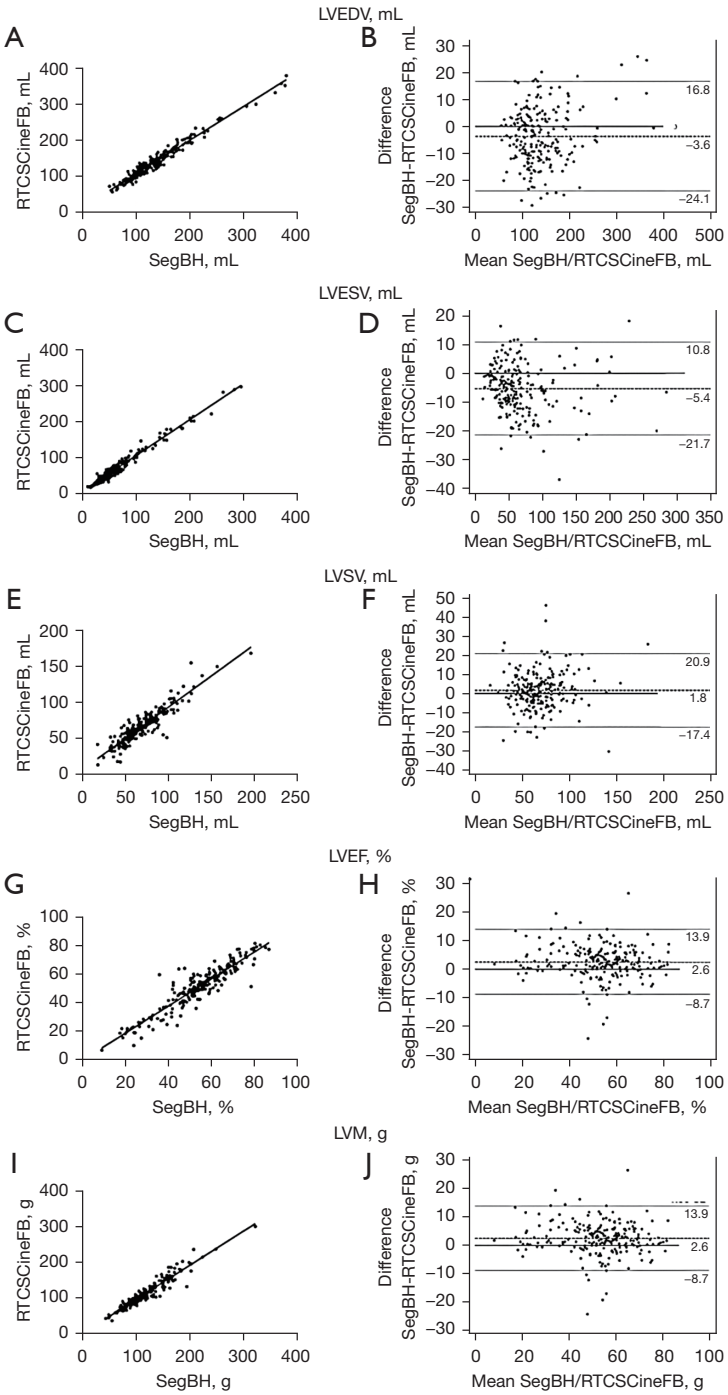

Figure 4 Scatter plots and modified Bland-Altman plots were used to assess the correlation and agreement between the LV function parameters and mass in both SegBH and RTCSCineFB images. The scatter plots demonstrated strong associations of LVEDV (A), LVESV (C), LVSV (E), LVEF (G), and LVM (I) obtained via the two methods. Modified Bland-Altman plots were generated to assess the agreement between the SegBH and RTCSCineFB images for various LV function parameters, including LVEDV (B), LVESV (D), LVSV (F), LVEF (H), and LVM (J). Mean differences are represented by dashed lines; 95% limits of agreement are indicated by dotted lines. LVEDV, left ventricular end-diastolic volume; SegBH, breath-hold segmented cine; RTCSCineFB, real-time compressed sensing cine with free breathing; LVESV, left ventricular end-systolic volume; LVSV, left ventricular stroke volume; LVEF, left ventricular ejection fraction; LVM, left ventricular mass; LV, left ventricular.

Table 5 Numbers of individuals with corresponding EF grades between the two methods

Parameters	RTCSCineFB			Total
	Grade 1	Grade 2	Grade 3	
SegBH				
Grade 1	33	0	1	34
Grade 2	8	23	6	37
Grade 3	1	22	130	153
Total	42	45	137	224

EF, ejection fraction; RTCSCineFB, real-time compressed sensing cine with free breathing; SegBH, breath-hold segmented cine.

Table 6 Kappa coefficients and reliability of EF grading

Parameters	SegBH *vs*. RTCSCineFB
κ	0.759
P	<0.001
95% CI	0.685–0.834

EF, ejection fraction; SegBH, breath-hold segmented cine; RTCSCineFB, real-time compressed sensing cine with free breathing; CI, confidence interval.

that this tendency arises from the lack of deep breaths by patients during the examination, as deep breathing increases lung volume and slightly reduces LV output, potentially influencing LVSV and LVEF measurements and leading to underestimations. However, these differences remain within clinically acceptable limits. The lower spatial and temporal resolutions of high-speed cine CMR, compared to standard cine CMR, may also contribute to overestimation of LVESV, particularly in patients with elevated heart rates (25). Further, the use of CS methods for LVM assessment may underestimate LVM due to image blurring or artifacts that hinder the accurate identification of endocardial and epicardial boundaries. Considering the clinical relevance of transmural pressure changes, ventricular filling, and output during breath holding, FB CS methods may provide more physiologically realistic data (26).

Our findings demonstrated robust consistency between the two methods in evaluating EF, with minimal changes observed in most cases. This consistency suggests that the accuracy of RTCSCineFB in quantitative EF grading is high, and this method is reliable even for patients with low or high EF values, and thus a suitable alternative for assessments of cardiac function when conventional imaging is not feasible. The ability to quantify and classify EF values strongly contributes to comprehensive cardiac evaluations and has clinical relevance in diagnostic decision making.

Limitations

This study had some important limitations. First, for the analysis of BMC, we only used images of the mid-ventricular level collected at the ED. Future studies should consider a more comprehensive evaluation of image quality via CS methods. Second, we solely focused on analyses of LV function and did not examine right ventricular function. Third, our study cohort only included patients with heart disease, and no quantitative analyses of healthy individuals were conducted. Our patient population also lacked diversity in terms of cardiac conditions. Fourth, the accurate delineation of endocardial and epicardial boundaries in quantitative studies of cardiac function was not possible for patients with poor image quality. As a result, cardiac function calculations could not be completed for these patients, and they were excluded from our study. These individuals typically experienced excessive motion artifacts due to their severe illness, which made it difficult for them to control their body movements. The inclusion of these cases might have introduced some bias into our findings. Finally, there were variations in certain parameters between the two methods studied; these differences may have a greater impact during the cardiac systolic period (12), which might have influenced our findings.

Conclusions

Based on our validation analyses using a large number of consecutive samples from patients with diverse clinical conditions, the CS methods offer a rapid and reliable imaging protocol and can be used to acquire images during FB, resulting in stable image quality with a significantly shorter scanning time. This stability advantage is particularly pronounced in individuals with arrhythmia. RTCSCineFB was found to be accurate in terms of evaluating LV function and exhibited strong consistency in EF grading. This scanning technique could be incorporated into clinical practice to efficiently acquire cardiac morphology without reducing diagnostic quality or diminishing data integrity.

Acknowledgments

Funding: This research was funded by the National Natural Science Foundation of China (No. 82272068).

Footnote

Reporting Checklist: The authors have completed the STROBE reporting checklist. Available at https://qims.amegroups.com/article/view/10.21037/qims-24-980/rc

Conflicts of Interest: All authors have completed the ICMJE uniform disclosure form (available at https://qims.amegroups.com/article/view/10.21037/qims-24-980/coif). J.A. was an employee of Siemens Shenzhen Magnetic Resonance throughout her involvement in the study. J.P. was an employee of Siemens Medical Solutions USA throughout his involvement in the study. The other authors have no conflicts of interest to declare.

Ethical Statement: The authors are accountable for all aspects of the work in ensuring that questions related to the accuracy or integrity of any part of the work are appropriately investigated and resolved. The study was conducted in accordance with the Declaration of Helsinki (as revised in 2013). The study protocol was approved by the Ethics Committee of Beijing Friendship Hospital (No. 2021-P2-418-01). All participants provided written informed consent to participate in the study.

References

1. Leiner T, Bogaert J, Friedrich MG, Mohiaddin R, Muthurangu V, Myerson S, Powell AJ, Raman SV, Pennell DJ. SCMR Position Paper (2020) on clinical indications for cardiovascular magnetic resonance. J Cardiovasc Magn Reson 2020;22:76.
2. Kramer CM, Barkhausen J, Bucciarelli-Ducci C, Flamm SD, Kim RJ, Nagel E. Standardized cardiovascular magnetic resonance imaging (CMR) protocols: 2020 update. J Cardiovasc Magn Reson 2020;22:17.
3. Deborde E, Dubourg B, Bejar S, Brehin AC, Normant S, Michelin P, Dacher JN. Differentiation between Fabry disease and hypertrophic cardiomyopathy with cardiac T1 mapping. Diagn Interv Imaging 2020;101:59-67.
4. Feng L, Benkert T, Block KT, Sodickson DK, Otazo R, Chandarana H. Compressed sensing for body MRI. J Magn Reson Imaging 2017;45:966-87.
5. Lustig M, Donoho D, Pauly JM. Sparse MRI: The application of compressed sensing for rapid MR imaging. Magn Reson Med 2007;58:1182-95.
6. Sridi S, Nuñez-Garcia M, Sermesant M, Maillot A, Hamrani DE, Magat J, Naulin J, Laurent F, Montaudon M, Jaïs P, Stuber M, Cochet H, Bustin A. Improved myocardial scar visualization with fast free-breathing motion-compensated black-blood T(1)-rho-prepared late gadolinium enhancement MRI. Diagn Interv Imaging 2022;103:607-17.
7. Longère B, Abassebay N, Gkizas C, Hennicaux J, Simeone A, Rodriguez Musso A, Carpentier P, Coisne A, Pang J, Schmidt M, Toupin S, Montaigne D, Pontana F. A new compressed sensing cine cardiac MRI sequence with free-breathing real-time acquisition and fully automated motion-correction: A comprehensive evaluation. Diagn Interv Imaging 2023;104:538-46.
8. Kocaoglu M, Pednekar AS, Wang H, Alsaied T, Taylor MD, Rattan MS. Breath-hold and free-breathing quantitative assessment of biventricular volume and function using compressed SENSE: a clinical validation in children and young adults. J Cardiovasc Magn Reson 2020;22:54.
9. Li Y, Lin L, Wang J, Cao L, Liu Y, Pang J, An J, Jin Z, Wang Y. Cardiac cine with compressed sensing real-time imaging and retrospective motion correction for free-breathing assessment of left ventricular function and strain in clinical practice. Quant Imaging Med Surg 2023;13:2262-77.
10. Scatteia A, Baritussio A, Bucciarelli-Ducci C. Strain imaging using cardiac magnetic resonance. Heart Fail Rev 2017;22:465-76.
11. Kido T, Kido T, Nakamura M, Watanabe K, Schmidt M, Forman C, Mochizuki T. Compressed sensing real-time cine cardiovascular magnetic resonance: accurate assessment of left ventricular function in a single-breath-hold. J Cardiovasc Magn Reson 2016;18:50.
12. Sudarski S, Henzler T, Haubenreisser H, Dösch C, Zenge

MO, Schmidt M, Nadar MS, Borggrefe M, Schoenberg SO, Papavassiliu T. Free-breathing Sparse Sampling Cine MR Imaging with Iterative Reconstruction for the Assessment of Left Ventricular Function and Mass at 3.0 T. Radiology 2017;282:74-83.
13. Liu J, Rapin J, Chang TC, Lefebvre A, Zenge M, Mueller E, Nadar MS. Dynamic cardiac MRI reconstruction with weighted redundant Haar wavelets. In: Proceedings of the Twentieth Meeting of the International Society for Magnetic Resonance in Medicine. Berkeley: International Society for Magnetic Resonance in Medicine. 2012:4249.
14. Allen BD, Carr M, Botelho MP, Rahsepar AA, Markl M, Zenge MO, Schmidt M, Nadar MS, Spottiswoode B, Collins JD, Carr JC. Highly accelerated cardiac MRI using iterative SENSE reconstruction: initial clinical experience. Int J Cardiovasc Imaging 2016;32:955-63.
15. Vincenti G, Monney P, Chaptinel J, Rutz T, Coppo S, Zenge MO, Schmidt M, Nadar MS, Piccini D, Chèvre P, Stuber M, Schwitter J. Compressed sensing single-breath-hold CMR for fast quantification of LV function, volumes, and mass. JACC Cardiovasc Imaging 2014;7:882-92.
16. Larson AC, Kellman P, Arai A, Hirsch GA, McVeigh E, Li D, Simonetti OP. Preliminary investigation of respiratory self-gating for free-breathing segmented cine MRI. Magn Reson Med 2005;53:159-68.
17. Longère B, Allard PE, Gkizas CV, Coisne A, Hennicaux J, Simeone A, Schmidt M, Forman C, Toupin S, Montaigne D, Pontana F. Compressed Sensing Real-Time Cine Reduces CMR Arrhythmia-Related Artifacts. J Clin Med 2021;10:3274.
18. Schulz-Menger J, Bluemke DA, Bremerich J, Flamm SD, Fogel MA, Friedrich MG, Kim RJ, von Knobelsdorff-Brenkenhoff F, Kramer CM, Pennell DJ, Plein S, Nagel E. Standardized image interpretation and post-processing in cardiovascular magnetic resonance - 2020 update : Society for Cardiovascular Magnetic Resonance (SCMR): Board of Trustees Task Force on Standardized Post-Processing. J Cardiovasc Magn Reson 2020;22:19.
19. Zange L, Muehlberg F, Blaszczyk E, Schwenke S, Traber J, Funk S, Schulz-Menger J. Quantification in cardiovascular magnetic resonance: agreement of software from three different vendors on assessment of left ventricular function, 2D flow and parametric mapping. J Cardiovasc Magn Reson 2019;21:12.
20. Kido T, Kido T, Nakamura M, Watanabe K, Schmidt M, Forman C, Mochizuki T. Assessment of Left Ventricular Function and Mass on Free-Breathing Compressed Sensing Real-Time Cine Imaging. Circ J 2017;81:1463-8.
21. Wang J, Lin Q, Pan Y, An J, Ge Y. The accuracy of compressed sensing cardiovascular magnetic resonance imaging in heart failure classifications. Int J Cardiovasc Imaging 2020;36:1157-66.
22. Zou Q, Xu HY, Fu C, Zhou XY, Xu R, Yang MX, Yang ZG, Guo YK. Utility of single-shot compressed sensing cardiac magnetic resonance cine imaging for assessment of biventricular function in free-breathing and arrhythmic pediatric patients. Int J Cardiol 2021;338:258-64.
23. Haubenreisser H, Henzler T, Budjan J, Sudarski S, Zenge MO, Schmidt M, Nadar MS, Borggrefe M, Schoenberg SO, Papavassiliu T. Right Ventricular Imaging in 25 Seconds: Evaluating the Use of Sparse Sampling CINE With Iterative Reconstruction for Volumetric Analysis of the Right Ventricle. Invest Radiol 2016;51:379-86.
24. Lin ACW, Strugnell W, Riley R, Schmitt B, Zenge M, Schmidt M, Morris NR, Hamilton-Craig C. Higher resolution cine imaging with compressed sensing for accelerated clinical left ventricular evaluation. J Magn Reson Imaging 2017;45:1693-9.
25. Miller S, Simonetti OP, Carr J, Kramer U, Finn JP. MR Imaging of the heart with cine true fast imaging with steady-state precession: influence of spatial and temporal resolutions on left ventricular functional parameters. Radiology 2002;223:263-9.
26. Treutlein C, Zeilinger MG, Dittrich S, Roth JP, Wetzl M, Heiss R, Wuest W, May MS, Uder M, Rompel O. Free-Breathing and Single-Breath Hold Compressed Sensing Real-Time MRI of Right Ventricular Function in Children with Congenital Heart Disease. Diagnostics (Basel) 2023;13:2403.

Cite this article as: Wang Z, Wang Z, An J, Yuan Y, Pang J, He Y. Cardiac compressed sensing real-time cine for the assessment of left ventricular function: a large sample size analysis. Quant Imaging Med Surg 2024;14(12):8785-8797. doi: 10.21037/qims-24-980

